Journal of Organometallic Chemistry, 331 (1987) 397–407
Elsevier Sequoia S.A., Lausanne – Printed in The Netherlands

Bonding in the ground state and excited states of copper–alkene complexes

P.H.M. Budzelaar *

Laboratory for Inorganic Chemistry, Eindhoven University of Technology, Eindhoven (The Netherlands)

P.J.J.A. Timmermans, A. Mackor

Institute of Applied Chemistry, TNO, Utrecht (The Netherlands)

and E.J. Baerends

Theoretical Chemistry Group, Free University, Amsterdam (The Netherlands)

(Received March 9th, 1987)

Abstract

The ground state and $^1B_2$ excited state of $Cu(C_2H_4)^+$ and of $CuX(C_2H_4)$ ($X = F$, Cl) have been investigated by the Hartree–Fock–Slater (HFS) method. The main metal–ligand interactions in the ground state are ethene $\pi \rightarrow$ Cu $4s$ donation and Cu $3d_\pi \rightarrow$ ethene π^* backdonation, which have comparable contributions to the metal–ligand bond strength. The excitation of $CuX(C_2H_4)$ does not involve an alkene $\pi \rightarrow$ metal charge transfer (LMCT), but instead is metal $3d \rightarrow$ alkene π^* charge transfer (MLCT) in character. The implications for the photochemistry of olefin–copper(I) complexes are discussed.

Introduction

The bonding between an olefin and a transition metal is usually described in a qualitative fashion in terms of the Dewar–Chatt–Duncanson model [1], in which there are two synergic alkene–metal bonding interactions: ligand-to-metal σ-donation (Fig. 1a) and metal-to-ligand π-backdonation (Fig. 1b). For the particular case of a copper(I)–olefin complex, the metal orbitals most involved in the bonding will be the Cu $4s$ σ-acceptor and the $3d_\pi$ π-donor orbitals. No general agreement exists on the relative importance of the σ-bonding and π-backbonding interactions. Restricted Hartree–Fock (RHF, [2]) calculations on $Cu(C_2H_4)^+$ by Kelber [3], Bögel [4] and Merchan [5] all indicated a negligible contribution of backbonding. On the other hand, Ziegler and Rauk [6] concluded from Hartree–Fock–Slater (HFS, [7]) calculations on $Cu(C_2H_4)^+$ that π-backbonding forms an important

0022-328X/87/$03.50

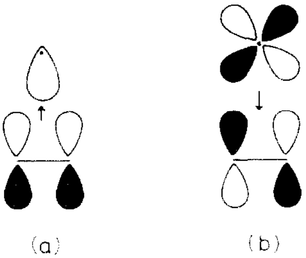

Fig. 1. Schematic representation of the ethene $\pi \rightarrow$ Cu $4s$ bonding (a) and Cu $3d_{\pi} \rightarrow$ ethene $\pi^{\star}$ backbonding (b) interactions.

contribution to the total interaction energy, and the infrared spectrum of $CuCl(C_2H_4)$ has been interpreted as indicating significant backbonding [8]. Kochi et al. [9] inferred from ^{13}C and ^{1}H NMR data that the relative contributions of bonding and backbonding depend on the olefin involved. Thus, for complexes of the type CuOTf(polyolefin)$_n$ (OTf = $CF_3SO_3^-$ = triflate; polyolefin = 1,5-cyclooctadiene, 1,3,5,7-cyclooctatetraene, norbornadiene or 1,5,9-cyclododecatriene) a downfield shift (deshielding) was found for the sp^2 carbons and the olefinic protons, indicating predominant σ-donation. Complexes of CuOTF with monoolefins (e.g. norbornene, cyclooctene) exhibited the reverse trend, which was taken as evidence for predominant π-backdonation.

Apart from differences in the theoretical procedures employed, the choice of a model system is expected to be important here. The relative amounts of bonding and backbonding depend critically on the relative energies of the orbitals of metal and ligand. The use of Cu^+ as a model for copper(I) salts results in an artificial stabilization of all copper levels, which favors σ-bonding but opposes π-backbonding. We have attempted to resolve the controversy by carrying out calculations on $Cu(C_2H_4)^+$ and on two more realistic model systems, viz. $CuF(C_2H_4)$ and $CuCl(C_2H_4)$. The HFS method was employed, but the copper basis set was of a slightly better quality than that used by Ziegler and Rauk [6].

Both bonding and backbonding influence the reactivity of a coordinated alkene molecule in the ground state as well as in the excited state. The use of copper(I) salts as catalysts for photochemical reactions of olefins is well-documented [10], but the precise role of the copper ion in these reactions has not been unequivocally established. Even the nature of the UV absorptions of the various copper(I)–alkene complexes at around 250 nm remains uncertain. Various explanations involving ligand-to-metal charge-transfer (LMCT) or metal-to-ligand charge-transfer (MLCT) as well as intra-ligand (IL) transitions have been put forward [10]; in addition, a mainly metal-centered $3d \rightarrow 4s$ transition (MM) would also be possible. These possibilities are summarized in Fig. 2. The previous ab-initio RHF studies [3–5] all agree on the level sequence Cu $3d <$ ethene $\pi <$ Cu $4s <$ ethene $\pi^{\star}$, which suggests that the lowest excited state is $^1A_1$ ($\pi \rightarrow 4s$), corresponding to a LMCT. However, the frequent breakdown of Koopman's theorem for organometallic complexes makes this conclusion somewhat premature [11]. Moreover, the presence of a counterion will have a large effect on the level ordering and may well change the nature of the lowest excited state.

In this work, we present a case for the Cu $3d \rightarrow$ alkene $\pi^{\star}$ MLCT as the

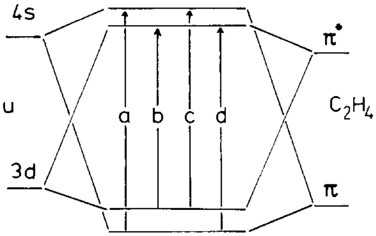

Fig. 2. Schematic representation of the four possible excitations in copper–alkene complexes: (a) LMCT, ligand-to-metal charge-transfer; (b) MLCT, metal-to-ligand charge-transfer; (c) MM, metal-to-metal excitation; (d) IL, intra-ligand excitation.

lowest-energy excitation in copper(I)–alkene complexes, and discuss the implications of the proposal for the photochemistry of such complexes.

Methods

The geometries assumed for all calculations are listed in Table 1; they are based on literature data for CuF, CuCl [12] and various copper(I)–alkene complexes [13]. The HFS series of programs have been described by Baerends et al. [7]. In all calculations the cores of the non-hydrogen atoms were kept frozen (up to 1*s* for C and F, 2*p* for Cl and 3*p* for Cu). The valence basis was of the double-ζ type, except for the copper 3*d* basis which was of triple-ζ quality. Exponents of the (Slater-type) basis functions are given in Table 1. Similar calculations on $Cu(C_2H_4)_2{}^+$ and

(Continued on p. 402)

Table 1

Basis sets and geometries

Slater exponents								
Cu	1*s*	24.45 [a]	C	1*s*	5.40 [a]	H	1*s*	0.76, 1.28
	2*s*	8.35 [a]		2*s*	1.24, 1.98	Cl	1*s*	14.55 [a]
	2*p*	11.71 [a]		2*p*	0.96, 2.20		2*s*	5.60 [a]
	3*s*	6.60 [a]	F	1*s*	8.33 [a]		2*p*	6.65 [a]
	3*p*	4.53 [a]		2*s*	1.92, 3.22		3*s*	1.75, 2.90
	3*d*	1.28, 3.10, 6.90 or [b] 1.65, 5.10		2*p*	1.48, 3.52		3*p*	1.30, 2.45
	4*s*	1.00, 1.90						
	4*p*	1.00, 1.90						

Geometrical details

Cu–F	1.743 Å
Cu–Cl	2.15 Å
Cu–(C=C)	1.97 Å
C=C	1.345 Å
C–H	1.04 Å
∠HCC	120°

In the calculations on $Cu(C_2H_4)^+$ and $CuX(C_2H_4)$, the ethene molecule is assumed to lie in the *xy*-plane with the carbon atoms on the *y* axis and the copper atom on the positive *z*-axis. In D_{2h} $Cu(C_2H_4)_2{}^+$, the ethene molecules are assumed to be parallel to the *xy*-plane with the carbon atoms in the *yz*-plane. In D_{3h} $Cu(C_2H_4)_3{}^+$ all ethene carbons are assumed to lie in the *xy*-plane.

[a] Inner-shell orbitals were kept frozen; these exponents were only used to ensure core-valence orthogonality. [b] Double-ζ set used for the calculations on $Cu(C_2H_4)_2{}^+$ and $Cu(C_2H_4)_3{}^+$.

Table 2

Orbital compositions for $Cu(C_2H_4)^{+\,a}$

Orbital	$-\epsilon_i$ (eV)	Description	Composition (%)											ρ (Cu–C_2H_4)
			Cu								ethene			
			$3d_\sigma$	$3d_{\pi x}$	$3d_{\pi y}$	$3d_\delta$	$4s$	$4p_\sigma$	$4p_{\pi x}$	$4p_{\pi y}$	σ	π	π^*	
$1a_1$	25.11	ethene σ	1				2	1			95	1		0.0343
$1b_2$	19.90	ethene σ			1					1	98			0.0137
$1b_1$	17.41	ethene σ		2					1		97			0.0185
$2a_1$	15.85	ethene σ	2								96	1		0.0102
$1a_2$	14.10	ethene σ				3					97			0.0092
$3a_1$	13.83	eth. $\pi + 4s$	18				12	2			5	64		0.0232
$2b_2$	12.33	$3d_{\pi y}$ + eth. π^*			93						2		5	−0.0032
$2b_1$	11.96	$3d_{\pi x}$		98							2			−0.0203
$2a_2$	11.87	$3d_\delta$				97					3			−0.0096
$4a_1$	11.72	$3d_\sigma$	84				7	1			4	8		0.0135
$5a_1$	11.67	$3d_\sigma$	93				2				1	3		−0.0006
$6a_1$	8.20	$4s$	2				77	14				8		−0.2486
$3b_2$	7.16	ethene π^*			5					25			70	0.0601
$3b_1$	4.88	$4p_{\pi x}$							102					−0.1324

[a] $1a_1$–$5a_1$ are doubly occupied (in the ground state).

Table 3

Mulliken population analyses

Complex (ν_{exc})	State	Gross populations														ρ(CuX–C_2H_4)	Gross charges		
		Cu								ethene			X				X	Cu	C_2H_4
		$3d_\sigma$	$3d_{\pi x}$	$3d_{\pi y}$	$3d_\delta$	$4s$	$4p_\sigma$	$4p_{\pi x}$	$4p_{\pi y}$	σ	π	π^*	σ	π_x	π_y				
$Cu(C_2H_4)^+$	Ground state	3.97	2.01	1.89	2.01	0.46	0.08	0.01	0.01	9.91	1.53	0.10				0.1776		+0.56	+0.44
(215 nm)	$^1B_2$ singlet	3.48	2.01	1.98	2.02	0.45	0.08	0.03	0.36	9.87	1.09	0.68				0.2129		+0.64	+0.36
$CuF(C_2H_4)$	Ground state	3.82	2.02	1.82	2.00	0.68	0.15	0.08	0.09	9.95	1.66	0.24	3.73	1.91	1.88	−0.0464	−0.53	+0.31	+0.22
(274 nm)	$^1B_2$ singlet	3.29	2.05	2.01	2.01	0.54	0.16	0.05	0.46	9.88	1.53	0.74	3.55	1.94	1.95	0.1326	−0.41	+0.55	−0.12
$CuCl(C_2H_4)$	Ground state	3.93	2.03	1.85	2.00	0.71	0.17	0.08	0.09	9.94	1.67	0.19	3.56	1.88	1.84	−0.0120	−0.35	+0.12	+0.24
(260 nm)	$^1B_2$ singlet	3.46	2.04	2.02	2.01	0.58	0.19	0.07	0.36	9.89	1.57	0.70	3.28	1.90	1.91	0.1276	−0.15	+0.25	−0.12

Complex	Donation		Backdonation $3d \rightarrow \pi^*$	q(Cu)
	$\pi \rightarrow 4s$	$\pi \rightarrow 4p$		
$Cu(C_2H_4)^+$	0.46	0.08	0.11	+0.56
$Cu(C_2H_4)_2{}^+$	0.61	0.18	0.08	+0.21
$Cu(C_2H_4)_3{}^+$	0.63	0.35	0.19	+0.15
$CuF(C_2H_4)$	(0.34)		0.24	+0.31
$CuCl(C_2H_4)$	(0.33)		0.19	+0.12

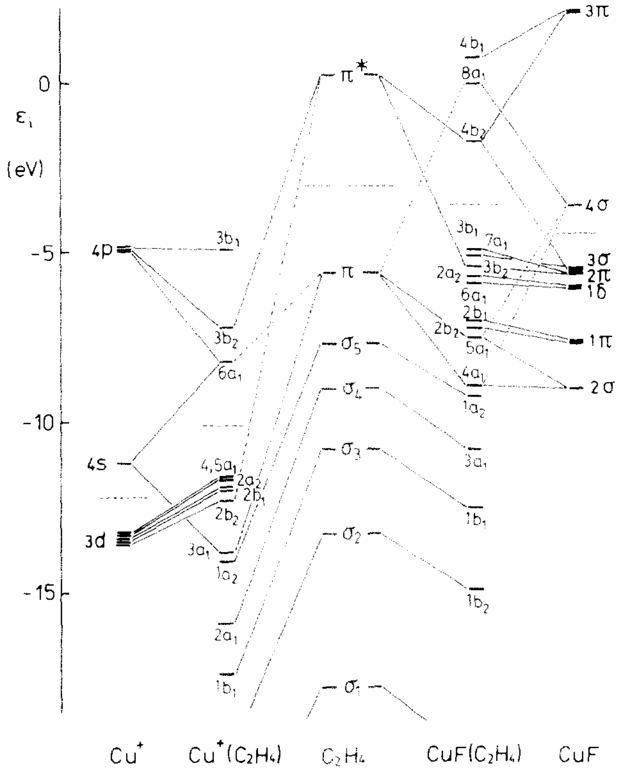

Fig. 3. HFS one-electron levels for the formation of $Cu(C_2H_4)^+$/$CuF(C_2H_4)$ from C_2H_4 and Cu^+/CuF. In all copper species, the five highest occupied orbitals (e.g., 1δ, 2π and 3σ in CuF) are predominantly Cu 3*d* in character.

$Cu(C_2H_4)_3{}^+$ were carried out with a basis having only two Cu 3*d* Slaters; therefore, the one-electron levels for these species are not directly comparable to those of $Cu(C_2H_4)^+$. The overall bonding picture is, however, quite similar for the three ions.

Restricted HFS calculations were carried out on the $^1A_1$ ground states, whereas the unrestricted HFS formalism was used for the $^1B_2$ singlet excited states [14]. Table 2 shows the orbital compositions for $Cu(C_2H_4)^+$; population analyses for all

Table 4

Electronic parts of the $CuX{-}C_2H_4$ interaction energies (kcal/mol) [a]

Symmetry	$Cu(C_2H_4)^+$	$CuF(C_2H_4)$	$CuCl(C_2H_4)$
a_1 (donation)	32.0	17.8	17.6
a_2	1.6	0.6	0.7
b_1	2.9	2.4	2.0
b_2 (backdonation)	15.8	23.6	20.9

[a] These data do not include exchange repulsion ("steric") terms, so they should not be interpreted as total $CuX{-}C_2H_4$ bond energies.

complexes are collected in Table 3. Figure 3 illustrates the formation of $Cu(C_2H_4)^+$ and $CuF(C_2H_4)$ from ethene and Cu^+ or CuF fragments. Interaction and excitation energies were calculated by Ziegler's transition-state method [15]; the energy compositions are given in Table 4.

The bonding in $Cu(C_2H_4)^+$

The formation of $Cu(C_2H_4)^+$ from Cu^+ and C_2H_4 fragments is illustrated in Fig. 3. All copper levels are raised, and orbitals on the ethene fragment lowered, because of their interaction with the electrostatic field of the other fragment. This effect is reinforced by a massive charge-transfer (0.44 e) from ethene to Cu^+. Most of this transfer comes from the ethene $\pi \rightarrow$ Cu 4*s* donation, which amounts to nearly 0.5 *e*. The interaction with the higher-lying Cu $4p_\sigma$ orbital is less important (≈ 0.08 *e*); the backdonation of Cu $3d_\pi$ into the ethene π^*-orbital is also rather small (≈ 0.10 *e*). The deformation density (Fig. 4a) clearly shows the dominance of the ethane $\pi \rightarrow$ Cu 4*s* σ-bonding interaction.

In complexes with two or three ethene molecules, the bonding picture is rather similar. Again, the most important interaction is the $\pi \rightarrow 4s$ donation, which results in a large overall charge transfer. A clear saturation effect is seen on going from $Cu(C_2H_4)^+$ via $Cu(C_2H_4)_2{}^+$ to $Cu(C_2H_4)_3{}^+$; the copper ion becomes a poorer acceptor as it accumulates more and more 4*s* electron density. Backdonation remains small, amounting to ≈ 0.1 *e* per *d*-orbital involved (d_{yz} for $n = 2$; d_{xy} and $d_{x^2-y^2}$ for $n = 3$).

The bonding in $CuX(C_2H_4)$

The bonding in the complexes of ethene with CuF and CuCl might be expected to resemble that in $Cu(C_2H_4)^+$. However, inspection of Table 3 and Fig. 3 reveals

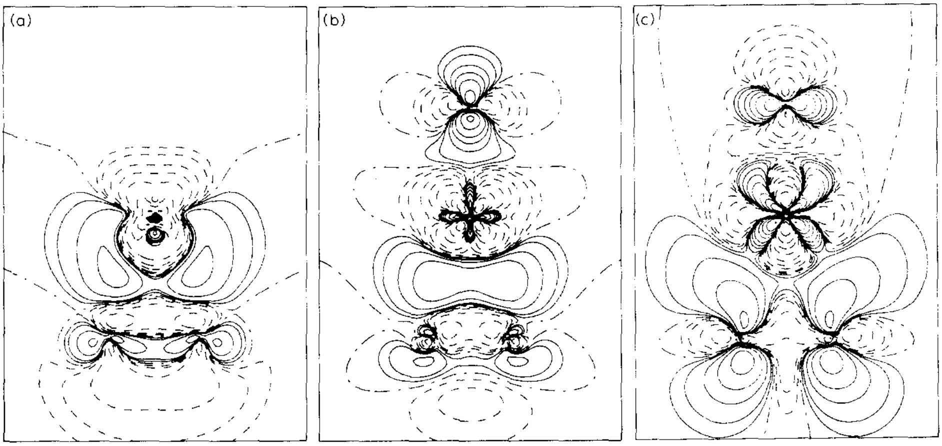

Fig. 4. Density difference plots for (a) the formation of $Cu(C_2H_4)^+$ from Cu^+ and C_2H_4; (b) the formation of $CuF(C_2H_4)$ from CuF and C_2H_4; (c) $7a_1 \rightarrow 4b_2$ (MLCT) excitation of $CuF(C_2H_4)$. Contour lines have been drawn at 0, 0.001, 0.002, 0.005, 0.01, 0.02, 0.05, 0.1, 0.2 and 0.5 e/au^3; dashed contours represent regions of decreased electron density.

some characteristic differences. Firstly, the charge on Cu^+ results in a large stabilization of all copper levels, which is only partly removed on complexation with ethene. Even in $Cu(C_2H_4)^+$, however, the metal $3d$ levels are located slightly above the ethene π-orbital. In the CuX complexes, the artificial stabilization of the copper levels is absent, and now the $3d$ levels are well above all filled ethene orbitals. In the HFS method, excitation energies can be approximated by orbital energy differences [16 *], so the level orderings give a strong indication that the Cu $3d$ levels will be important in photochemical processes (vide infra).

Another difference with the Cu^+ complex is found in the relative amounts of $\pi \rightarrow 4s$ donation and $3d_\pi \rightarrow \pi^*$ backdonation. Donation is decreased in the CuX complexes, because of the smaller initial charge on Cu. On the other hand, backdonation is not so much "uphill" in this case, and is found to be almost twice as large as in $Cu(C_2H_4)^+$. The energy decompositions in Table 4 show the same trend. Whereas in $Cu(C_2H_4)^+$ the contribution of the backdonation is minor ($\approx 30\%$), it actually constitutes more than half of the electronic interaction energy in $CuX(C_2H_4)$. Thus, one can really speak of synergic bonding–backbonding for the CuX complexes, in accordance with various experimental observations on copper(I)–alkene complexes [8,9]. This is also nicely illustrated by the deformation density (Fig. 4b) for the formation of $CuF(C_2H_4)$ from CuF and C_2H_4 fragments. The increase in electron density in the interfragment region and the depletion of charge from the Cu $3d_\pi$ orbital are clearly shown. Obviously, $Cu(C_2H_4)^+$ is not a realistic model for a detailed analysis of copper–alkene bonding. Some counterion has to be present, but its exact nature does not seem to be important in our monomeric model systems, since the results for the CuF and CuCl complexes are almost the same.

The nature of the lowest excited state

What is the nature of the lowest singlet excited state of copper(I)–olefin complexes? The previous RHF calculations [3–5] would suggest a $^1A_1$ ($\pi \rightarrow 4s$) LMCT excited state. Since Koopman's theorem frequently breaks down for organotransition metal complexes, however, separate calculations on various excited states would be needed for a definitive answer. HFS calculations generally show much smaller reorganization effects, so that the ordering of HFS one-electron levels usually provides a reliable indication of the lowest excited state [16 *].

In both $Cu(C_2H_4)^+$ and $CuX(C_2H_4)$, the ethene π-orbital ends up below the copper $3d$ levels (Fig. 3) and for the latter complexes the difference in orbital energies ($>$ 1 eV) virtually excludes the possibility of excitation from the π-orbital. The copper $3d$-orbitals are very close together, and the "excited" electron can come from any one of them. In order to check whether reorganization effects may favor excitation from the ethene π-orbital, we decided to carry out the excited-state calculations with the electron removed from the highest a_1 orbital. This orbital is predominantly Cu $3d_\sigma$ in character, but it has the same symmetry as the ethene π-orbital. If reorganization is important, it may change the nature of the half-empty orbital from Cu $3d_\sigma$ to ethene π. This effect is found to be minor for $CuX(C_2H_4)$:

---

* Reference number with asterisk indicates a note in the list of references.

according to the population analysis data in Table 3, the "excited" electron definitely comes from a Cu 3*d*-orbital and the ethene π-orbital contributes only 0.1 *e*.

Two virtual orbitals are candidates for receiving the "excited" electron: the a_1 Cu 4*s*-orbital (with considerable antibonding admixture from the ethene π-orbital) and the b_2 ethene $\pi^\star$-orbital (with some Cu $3d_\pi$ and $4p_\pi$ admixture). For $Cu(C_2H_4)^+$, the former is lower in energy, although the energy difference is fairly small. For the $CuX(C_2H_4)$ complexes, where the artificial stabilization of the Cu levels due to the positive charge is absent, the order is reversed, and the 4*s*-orbital is now more than 1 eV above the $\pi^\star$. Thus, the lowest excited state of $CuX(C_2H_4)$ will have an electron in the ethene $\pi^\star$-orbital, and not in the metal–ligand antibonding Cu 4*s*-orbital.

We arrive at the conclusion that the lowest excitations of copper(I)–alkene complexes will be of the Cu $3d \rightarrow$ alkene $\pi^\star$ MLCT type. Increase in the number of olefin ligands will result in an even stronger destabilization of the Cu 4*s*-level, so that our conclusions will also be valid for $CuX(olefin)_n$ complexes. However, complexes with very high-lying π levels (e.g. complexes of conjugated olefins) might have a $\pi \rightarrow \pi^\star$ excitation as the lowest-energy transition.

In the UV spectra of copper(I)–alkene complexes, several transitions around 254 nm occur with small energy differences [17]. Thus, the UV absorption of CuOTf(norbornene) has tentatively been assigned to an MLCT at 236 and an LMCT at 272 nm. The occurrence of several closely spaced transitions is readily accounted for by consideration of Fig. 3, where the five Cu 3*d* levels are close together. However, an LMCT ($\pi \rightarrow 4s$) in this part of the UV spectrum is hard to reconcile with our calculations.

Bonding in the excited state

A comparison of the gross fragment orbital populations for the ground state and excited state of $Cu(C_2H_4)^+$ (Table 3) shows that half of the "excited" electron comes from the ethene π-orbital, and the other half from the Cu $3d_\sigma$. The electron goes to a mixture of ethene $\pi^\star$ (60%) and Cu $4p_\pi$ (35%). The results for $CuX(C_2H_4)$ are different. Here, the electron comes largely from Cu $3d_\sigma$, with only small contributions (ca. 10% each) from the Cu 4*s*, the ethene σ-system, the fluorine atom and the ethene π-orbital; it still ends up in a mixture of ethene $\pi^\star$ (50%) and Cu $4p_\pi$ (35%). The excitation results in a depletion of charge at Cu, which is partly compensated for by a disappearance of the $3d_\pi \rightarrow \pi^\star$ backdonation. Nevertheless, the overall process is clearly MLCT. Figure 4c shows the electron redistribution accompanying the $7a_1 \rightarrow 4b_2$ excitation in $CuF(C_2H_4)$. The increase in ethene $\pi^\star$ and copper $3d_\pi$ density and the decrease of electron density in the Cu $3d_\sigma$ orbitals are clearly visible, as is a reorganization at the fluorine atom. Again, the presence of a counterion is seen to have a large influence, and its nature matters less, since the results for the two $CuX(C_2H_4)$ complexes (X = F, Cl) are virtually superimposable.

Relevance to photochemical processes

The copper(I)–alkene complexes involved in photochemical processes are always much more complicated than the simple model systems studied here. Factors neglected include association, substitution on the olefin, and coordination of solvent molecules. Most studies have been carried out with chlorides (which often act as bridging ligands, at least in the solid state [18]) or with the weakly coordinating triflate anion. We nevertheless feel that the conclusions derived above can, with some caution, be extrapolated to photochemically active copper(I)–alkene systems.

The processes most often encountered in the photochemistry of copper(I)–alkene complexes are [10]: *cis* ⇌ *trans* isomerization, dimerization [19 *], and skeletal rearrangement. Thus, upon irradiation of cyclohexene in the presence of CuOTf, three rearrangement products and three dimers are formed. Irradiation of the analogous norbornene complex gives two dimers in high yield. Dimerization is also observed in the copper(I)-catalyzed photocycloaddition of allyl alcohol to give 3-oxa-bicyclo[3.2.0]heptane via diallyl ether.

A variety of mechanisms have been invoked to explain the observed products; we will not attempt here to discuss the relative merits of these proposals [20] but the present calculations enable us to make some predictions about the first stage of the reaction. As discussed above, the initial photoproduct is probably a Cu $3d \rightarrow$ alkene π^* (MLCT) excited state. This leaves the copper atom with a hole in its *d*-shell, and it seems reasonable to assume that it will try to relieve this electron deficiency by forming a localized metal–carbon σ-bond, thus producing a 1,3-biradical species:

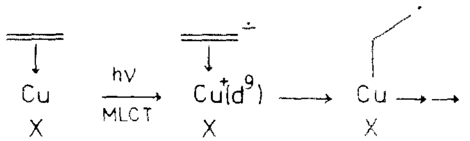

Ferraudi et al. [21] have recently reported spectroscopic evidence for the initial formation of such short-lived biradical species. Isomerization, dimerization and rearrangement can all be explained starting with such a biradical intermediate; this will be discussed more fully in a separate paper [22]. A final argument for the proposed mechanism is the fact that silver(I)–alkene complexes do not show the same or equally rich photochemistry (under exclusion of oxygen) as their copper(I) counterparts [23]. Ligand-to-metal transfer would be just as likely (or unlikely) there, but metal-to-ligand charge transfer would not be as easy for silver because the Ag 4*d* orbitals are much lower in energy than their Cu 3*d* counterparts.

Conclusions

Neither the ground state nor the excited states of copper(I)–alkene complexes are correctly modeled by $Cu(C_2H_4)^+$. A reasonable description requires some counterion, but its nature seems to be relatively unimportant. Backbonding in CuX–alkene complexes is much larger than in Cu^+ complexes and is by no means negligible. The photoexcitation of $CuX(C_2H_4)$ involves a metal-to-ligand $3d \rightarrow \pi^*$ transition, and this suggests a pathway for photochemical reactions of Cu^I–alkene complexes involving $Cu^{II}(d^9)$ biradical species.

Acknowledgements

This study was supported in part (P.J.J.A.T.) by the Netherlands Foundation for Chemical Research (SON) with financial aid from the Netherlands Organization for the Advancement of Pure Research (ZWO). The assistance of Mr. P. Vernooys is gratefully acknowledged.

References

1 M.J.S. Dewar, Bull. Soc. Chim. Fr., 18 (1951) C71; J. Chatt and L.A. Duncanson, J. Chem. Soc., (1953) 2939.

2 C.C.J. Roothaan, Rev. Mod. Phys., 23 (1951) 69.

3 J.A. Kelber, L.A. Harrah and J.R. Dennison, J. Organomet. Chem., 199 (1980) 281.

4 H. Bögel, Stud. Biophys., 93 (1983) 263.

5 M. Merchan, R. Gonzalez-Luque, J. Nebot-Gil and F. Thomas, Chem. Phys. Lett., 112 (1984) 412.

6 T. Ziegler and A. Rauk, Inorg. Chem., 18 (1979) 1558.

7 E.J. Baerends, D.E. Ellis and P. Ros, Chem. Phys., 2 (1973) 41; E.J. Baerends and P. Ros, Chem. Phys., 2 (1973) 52; E.J. Baerends and P. Ros, Chem. Phys., 8 (1975) 412.

8 M. Birgogne, J. Organomet. Chem., 160 (1978) 345.

9 R.G. Salomon and J.K. Kochi, J. Am. Chem. Soc., 95 (1973) 1880; J. Organomet. Chem., 64 (1974) 134.

10 See e.g. P.J. Kropp, Org. Photochem., 4 (1979) 1; R.G. Salomon, Tetrahedron, 39 (1983) 485; L. Moggi, A. Juris, D. Sandrini and M.F. Manfrin, Rev. Chem. Intermed., 4 (1981) 171; 5 (1984) 107; H. Hennig, D. Rehorek and R.D. Archer, Coord. Chem. Rev., 61 (1985) 1.

11 E.J. Baerends and P. Ros, Chem. Phys. Lett., 23 (1973) 391; M.M. Rohmer and A. Veillard, Chem. Phys., 11 (1975) 349; M.M. Rohmer and A. Veillard, J. Chem. Soc., Chem. Commun., (1973) 250; C. Famiglietti and E.J. Baerends, Chem. Phys., 62 (1981) 402.

12 Tables of Interatomic Distances and Configuration in Molecules and Ions, L.E. Sutton (Ed.), The Chemical Society, Spec. Publ., London, 1958.

13 See e.g. P.J.J.A. Timmermans, A. Mackor, A.L. Spek and B. Kojić-Prodić, J. Organomet. Chem., 276 (1984) 287; J.S. Thompson and J.F. Whitney, Acta Cryst., C40 (1984) 756; Inorg. Chem., 23 (1984) 2813; J.S. Thompson, R. Harlow and J.F. Whitney, J. Am. Soc., 105 (1983) 3522; M. Pasquali, C. Floriani, A. Gaetani-Manfredotti and A. Chiesi-Villa, Inorg. Chem., 18 (1979) 3535; J. Am. Chem. Soc., 100 (1978) 4918.

14 T. Ziegler, A. Rauk and E.J. Baerends, Theor. Chim. Acta, 43 (1977) 261.

15 T. Ziegler and A. Rauk, Theor. Chim. Acta, 46 (1977) 1.

16 Orbital energies in the HFS method do not correspond directly to ionization energies like they do in Hartree–Fock (Koopman's theorem). In general, they show a fairly uniform shift of ca. 5 eV with respect to experimental ionization energies; excitation energies correspond roughly to orbital energy differences. See e.g. T. Ziegler, A. Rauk and E.J. Baerends, Chem. Phys., 16 (1976) 209; E.J. Baerends and P. Ros, Chem. Phys. Lett., 23 (1973) 391.

17 R.G. Salomon and J.K. Kochi, J. Am. Chem. Soc., 96 (1973) 1889; D.J. Trecker, J.P. Henry and J.E. McKeon, J.A. Chem. Soc., 87 (1965) 3261; D.J. Trecker, R.S. Foote, J.P. Henry and J.E. McKeon, J. Am. Chem. Soc., 88 (1966) 3021; D.P. Schwendiman and C. Kutal, Inorg. Chem., 16 (1977) 719; J.Th. Evers, Ph.D. Thesis, Utrecht, 1979.

18 See e.g. T.C.W. Mak, H.N.C. Wong, K.H. Sze and L. Book, J. Organomet. Chem., 255 (1983) 123; P. Ganis, U. Lepore and E. Martuscelli, J. Phys. Chem., 74 (1970) 2439; J.H. van den Hende and W.C. Baird Jr., J. Am. Chem. Soc., 85 (1963) 1009; N.C. Baenziger, G.F. Richards and J.R. Doyle, Inorg. Chem., 3 (1964) 1529; N.C. Baenziger, H.L. Haight and J.R. Doyle, Inorg. Chem., 3 (1964) 1535.

19 Cyclotrimerization reactions have also been observed, but these are thermal reactions of an in situ prepared highly strained cycloalkene.

20 R.G. Salomon and J.K. Kochi, J. Am. Chem. Soc., 96 (1974) 1137; R.G. Salomon, K. Folting, W.E. Streib and J.K. Kochi, J. Am. Chem. Soc., 96 (1974) 1145; R.G. Salomon, Adv. Chem. Ser., 168 (1978) 174; J.Th. Evers, Ph.D. Thesis, Utrecht, 1979; T. Spee and A. Mackor, J. Am. Chem. Soc., 103 (1981) 6901; P.J.J.A. Timmermans, G.M.J. de Ruiter, A.H.A. Tinnemans and A. Mackor, Tetrahedron Lett., 24 (1983) 1419.

21 D. Geiger and A. Ferraudi, Inorg. Chim. Acta, 101 (1985) 197.

22 P.J.J.A. Timmermans et al., manuscript in preparation.

23 A.C. Angel, Ph.D. Thesis, University of Arizona, 1972; J.W. Bruno, T.J. Marks and F.D. Lewis, J. Am. Chem. Soc., 104 (1982) 5580; J.W. Bruno, Ph.D. Thesis, Northwestern University, Evanston, Illinois, 1983. The single example reported by Leh et al. (F. Leh, S.K. Wong and J.K.S. Wan, Can. J. Chem., 49 (1971) 2760) may have been an artefact.